



DAG-sensitive and Ca²⁺ permeable TRPC6 channels are expressed in dentate granule cells and interneurons in the hippocampal formation.

Journal:	<i>Hippocampus</i>
Manuscript ID:	HIPO-12-147.R1
Wiley - Manuscript type:	Research Article
Keywords:	Hippocampus, dendrite, GABAergic cell, feed-forward inhibition, feed-back inhibition

SCHOLARONE™
Manuscripts

Review

1
2
3 **DAG-sensitive and Ca²⁺ permeable TRPC6 channels are expressed in dentate granule**
4 **cells and interneurons in the hippocampal formation.**
5
6
7

8 Gergő A. Nagy¹, Gergő Botond¹, Zsolt Borhegyi¹, Nicholas W. Plummer², Tamás F. Freund¹
9 and Norbert Hájos¹
10

11 ¹Institute of Experimental Medicine, Hungarian Academy of Sciences, H-1450 Budapest,
12 Hungary

13 ²Laboratory of Neurobiology, National Institute of Environmental Health Sciences, NIH,
14 Research Triangle Park, North Carolina, USA
15
16

17
18 Abbreviated title: TRPC6 channels in the hippocampal formation.
19

20 Number of pages: 28

21 Number of figures: 7

22 Supplementary figures: 1
23
24

25 Correspondence:
26

27 **Norbert Hájos**
28

29 Institute of Experimental Medicine
30 Hungarian Academy of Sciences
31 Budapest, H-1450, Hungary
32 Phone: 36-12109400/387
33 Fax: 36-1-2109412
34 Email: hajos@koki.hu
35
36
37

38 Grant sponsor: Wellcome Trust International Senior Research Fellowship

39 Grant sponsor: National Office for Research and Technology

40 Grant number: OMFB-01678/2009

41 Grant sponsor: The Intramural Research Program of the NIH

42 Grant number: Z01-ES-101684
43
44

45 Key words: Hippocampus, dendrite, GABAergic cell, feed-forward inhibition, feed-back
46 inhibition
47
48
49
50
51
52
53
54
55
56
57
58
59
60

Abstract

Members of the transient receptor potential (TRP) cation channel family play important roles in several neuronal functions. To understand the precise role of these channels in information processing, their presence on neuronal elements must be revealed. In this study we investigated the localization of TRPC6 channels in the adult hippocampal formation. Immunostainings with a specific antibody, which was validated in *Trpc6* knockout mice, showed that in the dentate gyrus, TRPC6 channels are strongly expressed in granule cells. Immunogold staining revealing the subcellular localization of TRPC6 channels clarified that these proteins were predominantly present on the membrane surface of the dendritic shafts of dentate granule cells, and also in their axons, often associated with intracellular membrane cisternae. In addition, TRPC6 channels could be observed in the dendrites of some interneurons. Double immunofluorescent staining showed that TRPC6 channels were present in the dendrites of hilar interneurons and hippocampal interneurons with horizontal dendrites in the stratum oriens expressing mGlu_{1a} receptors, whereas parvalbumin immunoreactivity was revealed in TRPC6-expressing dendrites with radial appearance in the stratum radiatum. Electron microscopy showed that the immunogold particles depicting TRPC6 channels were located on the surface membranes of the interneuron dendrites. Our results suggest that TRPC6 channels are in a key position to alter the information entry into the trisynaptic loop of the hippocampal formation from the entorhinal cortex, and to control the function of both feed-forward and feed-back inhibitory circuits in this brain region.

Introduction

The hippocampal formation plays a crucial role in several cognitive functions, including coding and retrieval of information, as well as spatial navigation (Bird and Burgess, 2008). The neuronal circuits both in the dentate gyrus and in the hippocampus comprise excitatory principal neurons and inhibitory GABAergic cells (Freund and Buzsáki, 1996). While granule cells and hilar mossy cells are the excitatory neurons in the dentate gyrus, pyramidal cells compose the principal neurons in the hippocampus (Amaral et al., 1990). Inhibitory cells, however, are comparable in both regions (Freund and Buzsáki, 1996). The perisomatic region of principal neurons is innervated by fast spiking basket and axo-axonic cells containing the Ca^{2+} binding protein parvalbumin, as well as by regular spiking basket cells expressing the CB_1 cannabinoid receptor and the neuropeptide cholecystokinin (Freund and Katona, 2007). This neuropeptide can also be found in interneurons that synapse onto the dendrites of excitatory cells (Cope et al., 2002; Klausberger et al., 2005). The most distal part of the dendritic tree of principal neurons is innervated by GABAergic cells that express metabotropic glutamate receptor type 1 (mGlu_{1a}) and the neuropeptide somatostatin (Baude et al., 1993; Katona et al., 1999; Ferraguti et al., 2004). This latter cell type is an archetypal feed-back inhibitory cell, since the vast majority of their excitatory input originates from those principal cells that are innervated by these interneurons (Blasco-Ibanez and Freund, 1995; Maccaferri and McBain, 1995). Feed-forward inhibition in the hippocampal formation, however, has been proven to be predominantly accomplished by parvalbumin-containing interneurons, whose spiking is very effectively driven by feed-forward excitatory afferents (Glickfeld and Scanziani, 2006). Thus, distinct inhibitory cell types are specialized to control the different computational domains of principal neurons in the hippocampal formation (Miles et al., 1996; Lovett-Barron et al., 2012).

1
2
3 Cation channels mediating transient receptor potentials (TRP) are polymodal cellular
4 sensors, underlying several physiological functions (Ramsey et al., 2006). Overall, twenty
5 eight TRP channels, grouped into six subfamilies based on their sequence homology, have
6 been distinguished (Clapham, 2003; Owsianik et al., 2006). The members of the 'canonical'
7 subfamily, which exhibit a substantial Ca^{2+} permeability, have been shown to be activated by
8 a variety of distinct receptors, including tyrosine kinase TrkB receptors (TRPC3), mGlu_{1/5}
9 receptors (TRPC1, 5) or muscarinic cholinergic receptors (TRPC5) in the hippocampus
10 (Abramowitz and Birnbaumer, 2009; Bollimuntha et al., 2011). In addition, the role of the
11 latter channel type was proposed in the axonal growth of hippocampal pyramidal cells (Greka
12 et al., 2003).
13
14
15
16
17
18
19
20
21
22
23
24

25 Much less is known of TRPC6 channel function in the hippocampus, although a role
26 for these channels in dendritic growth and formation of excitatory synapses has been
27 postulated (Tai et al., 2008; Zhou et al., 2008). Other studies suggest that TRPC6 channels
28 might be involved in the synthesis of endocannabinoids (Bardell and Barker, 2010), which are
29 well-known retrograde messenger molecules (Katona and Freund, 2008; Kano et al., 2009).
30 Diacylglycerol (DAG), a precursor of endocannabinoids is known to promote the opening of
31 TRPC6 channels (Hofmann et al., 1999; Aires et al., 2007). An intriguing hypothesis is that
32 Ca^{2+} entering the neurons via TRPC6 channels upon DAG binding would trigger
33 endocannabinoid synthesis by activation of Ca^{2+} sensitive DAG lipase (Bisogno et al., 2003).
34 The localization of proteins involved in DAG synthesis (mGlu₅ receptors, phospholipase C) or
35 degradation (DAG lipase) on the spines receiving excitatory synapses was shown to be
36 predominantly present at the edge of asymmetric synapses (Lujan et al., 1996; Lujan et al.,
37 1997; Katona et al., 2006; Yoshida et al., 2006; Fukaya et al., 2008), forming a perisynaptic
38 annulus (Katona and Freund, 2008). Thus, if TRPC6 channels are a member of the molecular
39
40
41
42
43
44
45
46
47
48
49
50
51
52
53
54
55
56
57
58
59
60

1
2
3 machinery producing endocannabinoids, they should be found, at least in part, in the
4
5 perisynaptic annulus.
6

7
8 To obtain deeper insights into the potential role of TRPC6 channels in neuronal
9
10 operation, we aimed to identify the neuronal elements expressing these channels in the adult
11
12 hippocampal formation. Using immunocytochemical studies we found that dentate granule
13
14 cells and interneurons express TRPC6 channels, consistent with the *in situ* hybridization data
15
16 published by the Allen Institute for Brain Science (<http://mouse.brain-map.org>).
17
18

19 20 21 **Methods**

22 23 24 25 *Animal handling*

26
27
28
29 Experiments were performed according to the guidelines of the Institutional Ethical Codex
30
31 and the Hungarian Act of Animal Care and Experimentation (1998, XXVIII, section
32
33 243/1998), which conforms to the regulations of animal experiments of the European Union.
34
35 Animals were kept under a 12 h–12 h light–dark cycle, and water and food were available *ad*
36
37 *libitum*. All efforts were made to minimize pain and suffering and to reduce the number of
38
39 animals used. In this study, ten male Wistar rats (200–400g; Charles River, Hungary) and two
40
41 adult *Trpc6* knockout mice and their wild type littermates (n=2)(Dietrich et al., 2005) were
42
43 used.
44
45
46
47
48

49 50 51 *Immunohistochemistry*

52
53
54 The rats were deeply anaesthetized with an intraperitoneal injection of equitesin (4.2% w/v
55
56 chloral hydrate, 2.12% w/v MgSO₄, 16.2% w/w Nembutal, 39.6% w/w propylene glycol, and
57
58

1
2
3 10% w/w ethanol in H₂O) at a dosage of 0.2 ml/100 g body weight. Animals were perfused
4
5 through the heart sequentially with 4°C 0.9% NaCl for 2 min, fixative containing 2%
6
7 paraformaldehyde and 3.75% Acrolein in 0.1 M phosphate buffer (PB; pH = 7.4) for 10 min,
8
9 and fixative containing 2% paraformaldehyde in 0.1 M PB for 20 min. Mouse brains were
10
11 fixed by immersion in 4% paraformaldehyde. Coronal sections 40-50 µm in thickness were
12
13 cut using a Leica 1000S vibratome, cryoprotected in 30% sucrose in 0.1 M PB overnight, and
14
15 freeze thawed in an aluminium foil boat over liquid nitrogen to enhance the penetration of the
16
17 antibodies. After washing, the sections were treated with 0.1 M PB containing 1% sodium
18
19 borohydride for 10 min.
20
21

22
23 Sections then were transferred to a solution containing 2% bovine serum albumin
24
25 (BSA), 100 mg/ml glycine and 10% normal goat serum (Vector laboratories) in Tris-buffered
26
27 saline (TBS), pH 7.4, for 30 min, followed by incubation overnight at 4°C with a rabbit anti-
28
29 TRPC6 antibody (Alomone labs Ltd, Jerusalem, Israel) diluted 1: 20,000 in TBS. After
30
31 washing out the primary antibody, the sections were incubated in a biotinylated goat-anti
32
33 rabbit secondary antiserum (Vector Laboratories, Burlingame, CA) diluted 1:200 in TBS for 2
34
35 hours. Sections were then treated with a solution containing avidin-biotinylated horseradish
36
37 peroxidase complex (ABC Elite, Vector Laboratories) 1:300 in TBS for 2 hours, followed by
38
39 immunoperoxidase reaction using diaminobenzidine (DAB, Sigma-Aldrich, St Louis, MO) as
40
41 a chromogen.
42
43

44
45 For subcellular localization of TRPC6, we applied a pre-embedding immunogold
46
47 staining. In this case, the sections were incubated in the anti-TRPC6 antiserum (1:5000) for 2
48
49 days, followed by application overnight of a 1 nm gold-conjugated anti-rabbit secondary
50
51 antibody (Aurion, Wageningen, The Netherlands) diluted 1:50 in TBS containing 1% BSA,
52
53 0.1% fish gelatine and 100 mg/ml glycine. Sections were postfixed in 2% glutaraldehyde in
54
55 TBS and intensified with the Aurion R-Gent silver intensification kit.
56
57

1
2
3 All immunoperoxidase- and immunogold-stained sections were treated in 0.5% OsO₄
4 for 1 min, then in 1% OsO₄ for 15 min in 0.1 M PB followed by dehydration in an ascending
5 alcohol series and acetonitrile, and embedded in Durcupan. During dehydration, the sections
6
7 were treated with 1% uranyl acetate in 70% ethanol for 30 min. Finally, sections were re-
8
9 embedded and investigated in a light (Zeiss Axioscope 2) or an electron microscope (JEOL,
10
11 JEM-1011).
12
13
14
15

16 For confocal laser microscopy, we used a mixture of primary antisera of anti-TRPC6
17 (1:3000) and guinea pig anti-mGlu_{1a} (1:500; Frontier Institute co. Ltd, Japan; (Tanaka et al.,
18 2000)) or anti-TRPC6 (1:3000) and mouse anti-parvalbumin (1:2000; Sigma-Aldrich). The
19
20 sections were then incubated for 2 hours with a mixture of secondary antibodies diluted in
21
22 TBS: Alexa Fluor 488 goat anti-rabbit antibody (1:200, Molecular Probes, Eugene, OR) and
23
24 Alexa Fluor 594 goat anti-guinea pig (1:200, Molecular Probes), or Alexa Fluor 488 goat
25
26 anti-rabbit antibody (1:200, Molecular Probes) and Alexa Fluor 594 goat anti-mouse (1:200,
27
28 Molecular Probes). After washing, the sections were mounted on glass slides and covered in
29
30 Aqua poly/mount (Polysciences Inc., Warrington, PA, USA). Coverslips were sealed in nail
31
32 polish. Images were taken with a Nikon A1R confocal laser scanning microscope using a
33
34 sequential scanning mode.
35
36
37
38
39
40
41
42

43 *Quantitative analysis of the distribution of TRPC6 on the surface membrane of dentate*
44 *granule cells*
45
46
47
48

49 All quantifications have been performed on tissue samples derived from three rats and
50 pooled together, because there was no significant difference between animals ($p > 0.5$). For
51
52 analysis using ImageJ software (NIH), silver-intensified immunogold particles < 100 nm from
53
54 the cell membrane were counted as plasma membrane-attached. Images were taken from three
55
56
57
58
59
60

1
2
3 sequential ultrathin sections (cut using a Leica ultramicrotome) in the middle part of the
4
5 stratum moleculare or stratum granulosum at a magnification of 2500x. Calculation of particle
6
7 density was performed on the central image, in which all profiles were identified as spine,
8
9 dendrite, soma, axon ending or unknown profile using the two adjacent images. The number
10
11 of gold particles divided by the total length of the membranes was calculated for all those
12
13 dendrites, spines and somata measured in the central image whose profiles were not truncated
14
15 by the edge of the image. Since the distributions of immunogold labeling calculated on each
16
17 image were not different from normal distributions ($p < 0.01$), the mean and standard error of
18
19 the mean (SEM) of membrane-associated immunogold particles per 1 μm of the plasma
20
21 membrane were used to describe the distributions of immunolabeling in each compartment
22
23 (dendrites, spines and cell bodies).
24
25
26

27 To establish the distribution of TRPC6 labelling in spine heads, we counted 93
28
29 immunogold particles from each animal ($n=3$). Using methodology comparable to that
30
31 published earlier (Lujan et al., 1996; Lujan et al., 1997), we measured the distance along the
32
33 plasma membrane from the edge of the synaptic junction for each immunogold particle and
34
35 divided the data into 60 nm bins. The three datasets were not different from each other ($p > 0.5$,
36
37 Kruskal-Wallis non-parametric test), so the results were pooled.
38
39
40
41
42
43
44

45 Results

46 47 48 49 *Localization of TRPC6 channels in the rat hippocampal formation*

50
51
52
53
54 To get an overview of which neuronal elements express TRPC6 channels in the hippocampal
55
56 formation, we performed immunostaining using a polyclonal antibody developed against the
57
58
59
60

1
2
3 intracellular C-terminus loop of this transmembrane protein. In the rat tissue,
4
5 immunoperoxidase staining using DAB as a chromogen revealed a dark signal in the stratum
6
7 moleculare of the dentate gyrus and a fainter staining in the stratum lucidum of the CA3
8
9 subfield (Figure 1A, B, D). In the hilus and the stratum oriens of both hippocampal regions,
10
11 single dendrites (Figure 1C), in some cases decorated with long spines, could be observed
12
13 (Figure 6A, D). In addition, some smooth dendrites in the strata radiatum and oriens running
14
15 parallel with the pyramidal cell dendrites were also immunoreactive (Figure 1A). Outside of
16
17 the principal cell layer, cytoplasmic staining, including nuclear membrane labeling of some
18
19 neurons as well as staining of glia was also often apparent (Figure 1A, Supplementary figure
20
21 1).
22
23
24
25
26

27 *Localization of TRPC6 channels in the mouse hippocampal formation and the control of*
28
29 *antibody specificity using Trpc6 knockout mice*
30
31
32
33

34 To confirm the specificity of the immunostaining obtained with this antibody, we
35
36 compared the labeling in the hippocampus of wild type mice with that seen in *Trpc6* knockout
37
38 mice (Dietrich et al., 2005). In wild type mice, the pattern of the immunostaining for TRPC6
39
40 was identical to that seen in rats (Figure 2A); strong staining was apparent in the stratum
41
42 moleculare of the dentate gyrus and a fainter labeling in the stratum lucidum (Figure 2A, C).
43
44 Furthermore, the dendrites of interneurons localized in the strata oriens and radiatum of Cornu
45
46 Ammonis, as well as in the hilus, could be observed (Figure 2B). In contrast to this labeling
47
48 pattern, immunoreactivity in the strata moleculare and lucidum, as well as the
49
50 immunopositive dendrites in the hippocampal formation, was absent in *Trpc6* knockout mice
51
52 (Figure 2D, E, F). However, the cytoplasmic staining of neurons and the glial staining clearly
53
54 visible in all layers of the rat and mouse hippocampus was comparable in *Trpc6* knockouts
55
56
57
58
59
60

1
2
3 (Figure 2E, F; Supplementary figure 1). These results suggest that TRPC6 channels are
4 present in the input and output regions of dentate granule cells in addition to the dendrites of
5 interneurons, while the intracellular membrane signal and the glial staining seems to be non-
6 specific using this antibody.
7
8
9
10

11 12 13 14 *Subcellular distribution of TRPC6 channels in the dentate gyrus*

15
16
17
18 In the following sets of experiments, all investigations were carried out in the rat
19 hippocampal formation. We first examined the subcellular localization of TRPC6 channels in
20 the dentate gyrus. Using immunogold staining, we found that the labeling was predominantly
21 attached to the plasma membranes of the granule cells (Figure 3). To gain deeper insight into
22 the location of TRPC6 on the membrane surface of these excitatory cells, we compared the
23 density of immunogold particles in three different compartments (spines, dendrites and cell
24 bodies) by dividing the number of immunogold particles by the total membrane length of the
25 examined profiles. We found that the highest density of immunogold labeling was present in
26 the plasma membranes of the dendrites (0.12 ± 0.01 gold/ μm , $n=150$), with significantly
27 lower density on the surface of the spines (0.04 ± 0.01 gold/ μm , $n=267$) and cell bodies (0.06
28 ± 0.01 gold/ μm , $n=20$)(Figure 3). These results indicate that the dendrites of dentate granule
29 cells are preferentially equipped with TRPC6 channels.
30
31
32
33
34
35
36
37
38
39
40
41
42
43
44
45
46

47 *TRPC6 channels are evenly present on the surface membranes of dendritic spines with some*
48 *preference for the perisynaptic annulus around asymmetric synapses*
49
50
51

52
53
54 Although the density of TRPC6 channels was highest on dendritic shafts, we carried
55 out a more thorough investigation of the channel localization related to the excitatory
56
57
58
59
60

1
2
3 synapses on spines. The rationale behind this analysis was that some proteins (e.g. those that
4
5 are involved in the regulation of DAG levels on spines) are preferentially found at the edge of
6
7 synapses, forming a perisynaptic annulus (Katona and Freund, 2008). To establish whether
8
9 TRPC6 channels on the spines of dentate granule cells are members of the perisynaptic
10
11 annulus, we determined the sub-synaptic distribution of TRPC6 channels on spines in relation
12
13 to the synaptic junction. Following the procedure published by Lujan and colleagues (Lujan et
14
15 al., 1996; Lujan et al., 1997), we measured the distance of each immunogold particle from the
16
17 edge of the synapse, and sorted the values into 60 nm bins. This analysis revealed that TRPC6
18
19 channels occur evenly on the surface membranes of dendritic spines, with some preference for
20
21 the perisynaptic annulus around asymmetric synapses (Figure 4). Importantly, immunogold
22
23 particles were rarely observed within the postsynaptic density or intracellularly in the spine
24
25 cytoplasm (< 2%). These data imply that the presence of TRPC6 channels in dendritic spines
26
27 partially overlaps with the perisynaptic annulus, but the majority of labeling is more evenly
28
29 distributed on the surface membranes of spines.
30
31
32
33
34
35

36 *Subcellular localization of TRPC6 channels in the stratum lucidum of the CA3 subfield*

37
38
39
40 Since a weak, but obvious, immunolabeling was present in the stratum lucidum of both rats
41
42 and wild type mice but was absent in *Trpc6* knockout mice, we next investigated the
43
44 subcellular localization of these channel proteins in the termination zone of dentate granule
45
46 cells. In contrast to what we found in the stratum moleculare, namely that immunogold
47
48 particles depicting TRPC6 channels were preferentially attached to the plasma membranes of
49
50 dendrites and spines (Figure 3), the immunogold labeling in the stratum lucidum was often
51
52 present inside the axons in addition to being in the close vicinity of the axonal membranes
53
54 (Figure 5). These axons regularly formed bundles characteristic of mossy fibers, the axons of
55
56
57
58
59
60

1
2
3 dentate granule cells. In line with this notion, some immunogold particles could be seen in the
4
5 large mossy terminals, the specialized axon endings of dentate granule cells. In these
6
7 terminals, immunogold particles avoided the vesicular clusters, but were frequently associated
8
9 with intracellular membrane cisternae or the plasma membrane (Figure 5). These observations
10
11 indicate that, while TRPC6 channels of dendrites and spines of dentate granule cells were
12
13 almost exclusively present on the surface membranes, TRPC6 in the axons could often be
14
15 detected intracellularly, where the immunolabeling was occasionally associated with
16
17 membrane cisternae in mossy terminals.
18
19

20 21 22 *Interneurons expressing TRPC6 channels*

23
24
25
26
27 In the next set of experiments, we aimed to identify the interneurons whose dendrites
28
29 are immunoreactive for TRPC6 channels. The dense meshwork of dendrites at the border of
30
31 the stratum oriens and alveus, as well as in the hilus, resembled those interneuron dendrites
32
33 that express mGlu_{1a} receptors in the hippocampal formation. To prove that TRPC6 channels
34
35 are present on the dendrites of mGlu_{1a}-immunopositive interneurons, we performed double
36
37 immunofluorescent staining. The analysis unequivocally showed that the vast majority of
38
39 TRPC6-immunoreactive dendrites located both at the border of stratum oriens and alveus
40
41 (Figure 6A-C) and in the hilus (Figure 6D-F) were indeed labeled for mGlu_{1a}. Then, we
42
43 sought to clarify the neurochemical marker content of the smooth TRPC6-immunopositive
44
45 dendrites seen in the stratum radiatum of the CA1 region (Figure 1A). We chose to examine
46
47 the presence of parvalbumin in these dendrites, since this Ca²⁺ binding protein is expressed in
48
49 a large population of GABAergic cells in the hippocampal formation (Katsumaru et al., 1988;
50
51 Freund and Buzsáki, 1996). The analysis of double-immunofluorescence stained material
52
53 revealed that the majority of the smooth dendrites immunoreactive for TRPC6 were also
54
55
56
57
58
59
60

1
2
3 stained for parvalbumin in the hippocampus (Figure 6G-I). We could not examine the
4
5 presence of TRPC6 channels on the parvalbumin-immunopositive dendrites in the stratum
6
7 moleculare of the dentate gyrus, since no TRPC6-immunoreactive dendrite could be
8
9 distinguished in this layer, probably because this was masked by the dense immunostaining
10
11 for dendrites and spines (Figure 1B). These data collectively suggest that, in the hippocampal
12
13 formation, TRPC6 channels are expressed by at least two distinct interneuron populations,
14
15 one characterized by mGlu_{1a} expression, the other by parvalbumin content.
16
17

18
19
20
21 *TRPC6 channels are present on the plasma membranes of interneuron dendrites*
22
23

24
25 Finally, we investigated the subcellular localization of TRPC6 on the dendrites of
26
27 interneurons. Using preembedding immunogold staining, we found that immunogold particles
28
29 were attached to the surface plasma membrane of spiny interneuron dendrites both in the
30
31 stratum oriens and hilus (Figure 7A, B)(Baude et al., 1993; Acsády et al., 1998; Takacs et al.,
32
33 2012). Similarly, the aspiny dendrites densely covered by asymmetric synapses in the stratum
34
35 radiatum, resembling parvalbumin-immunoreactive dendrites (Gulyas et al., 1999), were also
36
37 decorated with immunogold particles associated with the plasma membrane (Figure 7C).
38
39 These results suggest that TRPC6 channels are in a position to control the input properties of
40
41 both mGlu_{1a}- and parvalbumin-expressing GABAergic cells in the hippocampal formation.
42
43
44
45
46
47
48

49 Discussion

50
51
52
53

54 We have found that in the hippocampal formation, TRPC6 channels are expressed by dentate
55
56 granule cells and inhibitory interneurons. Electron microscopic analysis revealed that TRPC6
57
58

1
2
3 channels are localized on the plasma membranes of the dendrites, spines and somata of
4
5 dentate granule cells, as well as on the surface membrane of interneuron dendrites. In
6
7 addition, a more detailed analysis showed that the TRPC6 labeling is evenly present in the
8
9 dendritic spines of dentate granule cells, with some preference for the edge of asymmetric
10
11 synapses. In the axons and axon terminals of dentate granule cells, TRPC6 channels were
12
13 regularly observed intracellularly, occasionally associated with membrane cisternae.
14
15

16
17
18 *TRPC6 channels on the plasma membrane of dentate granule cells*
19

20
21
22
23 Our immunocytochemical results showing that TRPC6 channels are abundant in the stratum
24
25 moleculare of the dentate gyrus confirm an earlier work using a different antibody developed
26
27 against TRPC6 (Chung et al., 2006). In that study, a strong immunolabeling in the stratum
28
29 moleculare was also described, but no labeling in the other layers of the hippocampus was
30
31 reported. Using the immunogold technique we have extended these earlier data by
32
33 demonstrating that in the stratum moleculare, TRPC6 proteins are present on the plasma
34
35 membrane of the spines and dendrites of dentate granule cells. Since the opening of these
36
37 channels is controlled by DAG (Hofmann et al., 1999; Aires et al., 2007), we sought to
38
39 compare the distribution of TRPC6 channels on spines with those proteins known to be
40
41 involved in the regulation of local DAG levels. Such quantitative data are available mainly for
42
43 a signaling cascade formed by mGlu₅, PLCβ1/4 and DAG lipase, which are present in the
44
45 perisynaptic annulus around asymmetric synapses (Lujan et al., 1996; Lujan et al., 1997;
46
47 Nakamura et al., 2004; Katona et al., 2006; Yoshida et al., 2006; Fukaya et al., 2008). Since
48
49 we found that a fraction of TRPC6 channels in the spines are located at the edge of
50
51 asymmetric synapses, this structural correlation with the location of mGlu₅-mediated DAG
52
53 production could imply that mGlu-dependent depolarization of dentate granule cells and the
54
55
56
57
58
59
60

1
2
3 parallel Ca^{2+} elevation may be, at least in part, mediated by TRPC6 channels. In addition to its
4
5 many other roles, Ca^{2+} entry via TRPC6 channels may also serve as a feedback signal to
6
7 terminate the channel operation (Hofmann et al., 1999). The activity of DAG lipase can be
8
9 markedly enhanced upon intracellular Ca^{2+} increase, which more effectively degrades DAG
10
11 and leads to the closure of this channel (Bisogno et al., 2003). Thus, PLC β 1-dependent DAG
12
13 production upon activation of mGlu₅ receptors and DAG degradation by DAG lipase are key
14
15 regulators of TRPC6 channel opening, and seem to be compartmentalized in the spines of
16
17 dentate granule cells. A similar scenario can be postulated to be present in the spines of
18
19 pyramidal cells, where other DAG-sensitive TRPC channels with less Ca^{2+} permeability than
20
21 TRPC6, such as TRPC3 and/or TRPC7 (Abramowitz and Birnbaumer, 2009; Bollimuntha et
22
23 al., 2011) can take part in mediating the mGlu-dependent depolarization (Gee et al., 2003). It
24
25 is important to highlight that each metabotropic receptor using the Gq protein to conduct its
26
27 function could probably activate TRPC6 and/or other DAG-sensitive TRPC channels. For
28
29 example, previous studies have shown that mGlu₁, TrkB or type 1 muscarinic receptors
30
31 operating via the Gq signaling pathway can be found on the spines of principal neurons
32
33 (Baude et al., 1993; Drake et al., 1999; Uchigashima et al., 2007; Yamasaki et al., 2010).
34
35 Thus, upon activation, all these metabotropic receptors may open DAG-sensitive TRPC
36
37 channels, mediating cation influx into the spines of cortical excitatory cells.
38
39
40
41
42

43 In addition to the spines, immunolabeling for TRPC6 channels was also localized to
44
45 the surface membrane of granule cell dendrites. Since all metabotropic receptors mentioned
46
47 above have also been found on the plasma membrane of granule cell dendrites or somata
48
49 (Baude et al., 1993; Lujan et al., 1996; Drake et al., 1999; Yamasaki et al., 2010), similar
50
51 mechanisms for opening TRPC6 channels are highly likely to occur in dendritic and somatic
52
53 compartments as well. Thus, the input domain of dentate granule cells is equipped with all
54
55 necessary building blocks for the regulation of TRPC6 channel function.
56
57
58
59
60

1
2
3 In addition to synapse formation and dendritic growth functions (Tai et al., 2008; Zhou
4 et al., 2008), TRPC6 channels may also have a role in controlling endocannabinoid
5 production, as proposed in a recent study (Bardell and Barker, 2010). These retrograde
6 signaling molecules are synthesized “on-demand” upon activation of DAG lipase, and can
7 effectively regulate transmitter release from axon terminals (Kano et al., 2009), serving as a
8 circuit-breaker at high activity levels (Katona and Freund, 2008). Since TRPC6 channels in
9 the presence of DAG can promote local Ca^{2+} increase, a necessary step for endocannabinoid
10 synthesis, these cation channels might be involved in synaptic plasticity mediated via CB_1
11 cannabinoid receptors (Katona and Freund, 2008; Kano et al., 2009).
12
13
14
15
16
17
18
19
20
21
22
23
24

25 *TRPC6 channels in the axons and terminals of dentate granule cells*

26
27
28
29 In contrast to that observed on the dendrites and spines of dentate granule cells, immunogold
30 labeling depicting TRPC6 channels in mossy fibers was frequently found intracellularly. This
31 observation suggests that in the axons of dentate granule cells, TRPC6 channels may play
32 different function(s) than in the input domain of these excitatory cells. Experimental evidence
33 suggests that TRPC channels could have a role in the regulation of Ca^{2+} levels in intracellular
34 stores (Cahalan, 2009; Pani et al., 2012). In agreement with this proposal, we have seen
35 immunogold labeling associated with membrane cisternae in mossy terminals, which might
36 indeed serve as Ca^{2+} stores. A recent study by Shimizu et al. (Shimizu et al., 2008) described
37 the subcellular localization of type 2 ryanodine receptors in the axons of dentate granule cells.
38 Similarly to what we have observed for TRPC6 channels, this type of ryanodine receptor was
39 prevalently localized intracellularly in the axons of granule cells, and less abundantly in the
40 mossy terminals, but avoided the vesicular clusters. Since this study elegantly showed that
41 ryanodine receptors could amplify the Ca^{2+} signal in mossy terminals in a use-dependent
42
43
44
45
46
47
48
49
50
51
52
53
54
55
56
57
58
59
60

1
2
3 manner, an intriguing hypothesis is that TRPC6 channels, if they are located on the same
4
5 axonal compartments as ryanoidne receptors, could have a function in the Ca^{2+} regulation in
6
7 mossy fibers, indirectly affecting the neurotransmitter release.
8
9

10 11 *TRPC6 channels in interneurons*

12
13
14
15
16 In addition to excitatory granule cells, inhibitory interneurons immunoreactive for mGlu_{1a} or
17
18 parvalbumin expressed TRPC6 channels on their dendritic membrane surface. Since both cell
19
20 types are equipped with mGlu₁ and/or mGlu₅ receptors (Baude et al., 1993; Lujan et al., 1996;
21
22 van Hooft et al., 2000; Topolnik et al., 2006), type 1 and/or 3 muscarinic receptors (Lawrence
23
24 et al., 2006; Cea-del Rio et al., 2010) and probably TrkB receptors (Holm et al., 2009) as well
25
26 as DAG lipase (our unpublished data), we suggest that signaling mechanisms comparable to
27
28 those in dentate granule cells could control the operation of TRPC6 channels in interneurons.
29
30 A recent study demonstrated that Ca^{2+} entry via TRP channels into cells resembling mGlu_{1a} -
31
32 immunoreactive interneurons with horizontal dendrites in the stratum oriens of the CA1
33
34 region contributes to the long-term enhancement of excitatory synaptic input onto these
35
36 interneurons (Topolnik et al., 2006). Although in this study the nature of the TRP channels
37
38 was not revealed, our data imply that TRPC6 channels with high Ca^{2+} permeability might
39
40 contribute to the control of synaptic plasticity observed in these interneurons. Given that the
41
42 two populations of GABAergic cells expressing TRPC6 channels take part in feed-back
43
44 (mGlu_{1a} -immunopositive interneurons) or feed-forward (parvalbumin-containing
45
46 interneurons) inhibitory loops, the activation of these DAG-sensitive TRPC channels could
47
48 alter information routing in hippocampal microcircuits (Pouille and Scanziani, 2004).
49
50
51
52
53
54
55
56
57
58
59
60

1
2
3 In summary, TRPC6 channels, upon activation of Gq-coupled metabotropic receptors, may
4
5 effectively regulate information processing in the first stage of the hippocampal trisynaptic
6
7 loop by affecting Ca^{2+} levels in dentate granule cells. In addition, these TRPC channels are in
8
9 a position to impact the operation of distinct interneuron types, likely playing a role in their
10
11 synaptic plasticity.
12

13
14
15
16
17
18 **Acknowledgements** We are grateful to Prof. Lutz Birnbaumer for generously providing
19
20 *Trpc6* knockout mice. We thank Rita Karlócai for helping with confocal images and Katalin
21
22 Lengyel for her excellent technical assistance. The authors also wish to thank Mr. László
23
24 Barna, the Nikon Microscopy Center at IEM, Nikon Austria GmbH and Auro-Science
25
26 Consulting Ltd for kindly providing microscopy support. The authors declare no conflict of
27
28 interest. This research was supported in part by the intramural research program of the NIH,
29
30 National Institute of Environmental Health Sciences.
31
32
33
34
35
36
37
38
39
40
41
42
43
44
45
46
47
48
49
50
51
52
53
54
55
56
57
58
59
60

Figure legends

Figure 1. Light micrographs of the rat hippocampal formation immunostained for TRPC6 protein. A: Low power micrograph showing a specific laminar distribution of TRPC6-immunostaining in the CA1 region and the dentate gyrus. A strong labeling can be seen in the stratum moleculare of the dentate gyrus in addition to numerous immunostained dendrites located both in the hilus and in strata oriens and radiatum. Moreover, some immunoreactive cell bodies resembling interneurons are distributed in all layers of the hippocampal formation. B: At higher magnification the dendrites of the dentate granule cells surrounded by a dense punctuated immunostaining are visible in the stratum moleculare. C: In CA1, a meshwork of neuronal processes can be found at the stratum oriens/alveus border formed mainly by horizontally running interneuronal dendrites. D: In the stratum lucidum of the CA3 subfield, while the main apical dendrites of CA3 pyramidal cells appear to be immunonegative, they are outlined by a dense immunostained neuropil. *alv.*, alveus; *o.*, stratum oriens; *p.*, stratum pyramidale; *rad.*, stratum radiatum; *l.m.*, stratum lacunosum-moleculare; *mol.*, stratum moleculare; *gr.*, stratum granulosum; *h.*, hilus. Scale bars: A, 100 μm ; B, C, 20 μm ; D, 100 μm .

Figure 2. Light microscopy of TRPC6 localization in the mouse hippocampal formation. A: Wild type mice have an identical TRPC6 localization pattern to rats. An intense staining is visible in the stratum moleculare of the dentate gyrus. The pattern of this immunoreaction is indistinguishable from that observed in the rat dentate gyrus shown at higher magnification (C). B: The meshwork of neuronal processes at the border of the stratum oriens/alveus stained for TRPC6 is also present in the mouse hippocampus, comparable to that seen in the rat. D: In contrast to wild type mice, immunostaining for TRPC6 was absent in the dentate gyrus in

1
2
3 *Trpc6* knockout mice (F). E: Similarly, the TRPC6-immunoreactive meshwork formed mainly
4 by interneuronal dendrites in CA1 was not visible in KO mice. However, the cell body
5 staining with this TRPC6 antibody was comparable both in wild type and *Trpc6* knockout
6 mice, indicating that this signal is unrelated to the presence of TRPC6 protein. Scale bars: A,
7 D, 500 μm ; B, C, E, F, 50 μm .

16 **Figure 3.** TRPC6 is expressed in the plasma membrane of the dendrites and spines of dentate
17 granule cells. A1-2: Consecutive electron micrographs taken in the stratum moleculare
18 demonstrate that immunogold particles representing TRPC6 proteins are present on the
19 plasma membranes of the dendrites (arrows) and spines (arrowheads) of dentate granule cells.
20 Note that the gold particles are attached to the intracellular surface of the plasma membrane,
21 in accord with the predicted position of the intracellular epitope of the TRPC6 protein
22 recognized by this antiserum. In addition, some gold particles could be occasionally seen
23 intracellularly (open arrowhead) that may represent channels during trafficking. Scale bars:
24 0.5 μm . B shows the immunogold density revealed on different membrane segments. There
25 was a significant difference in the density of immunolabeling on the surface of the dendrites
26 and somata (marked with *, $p=0.02$) and dendrites and spines (marked with **, $p=0.002$).
27 There was no difference in the density between spines and somata (n.s., non-significant,
28 $p=0.41$). The symbols and whiskers indicate the mean and SEM, respectively.

47 **Figure 4.** Distribution of TRPC6 on the spine heads of dentate granule cells. A, B: High-
48 resolution preembedding immunogold staining for TRPC6 demonstrates that this channel
49 protein is present on the spines (arrowheads) receiving asymmetric synapses, as well as on
50 dendrites with small diameter (arrows). C1-2: Consecutive sections of a labeled spine that
51 receives an asymmetric synapse. Scale bars: 0.2 μm . D: Relationship between the distance of

1
2
3 immunolabeling depicting TRPC6 and the half perimeter of extrasynaptic membrane of spines
4
5 (n=279). There is a population of labeling (~ 15%), indicated with a dashed line, which is
6
7 located at the edge of synapses. A larger fraction of the immunogold particles show an even
8
9 distribution on the surface membrane of spines. Bar graph on top; Spatial distribution of
10
11 immunogold particles in relation to the postsynaptic density (PSD) on spine heads. The
12
13 distance from the edge of the synaptic junction (position 0; open arrowheads in A-C) was
14
15 measured along the plasma membrane. The values were divided into 60 nm bins. Bar graph
16
17 on left; Distribution of the half lengths of the perimeters of spines excluding the synaptic
18
19 junction.
20
21
22
23
24

25 **Figure 5.** TRPC6 channels are often localized intracellularly in the axons of dentate granule
26
27 cells. A1-2: Gold particles representing TRPC6 channels were mainly found in the *en passant*
28
29 axons, frequently forming bundles in the stratum lucidum (arrowheads). In the mossy
30
31 terminals, gold labeling avoiding vesicular clusters was commonly attached to **the plasma**
32
33 **membrane** or intracellular membrane cisternae (arrows). Inserts show the same structure taken
34
35 from the bottom left parts of the consecutive sections, highlighting a gold particle attached to
36
37 an intracellular membrane cisterna. B, C, D: High-power electron micrographs demonstrating
38
39 immunogold staining associated with membrane cisternae (open arrows). Scale bars: A, 0.5
40
41 μm ; insert 0.25 μm ; B-D 0.2 μm .
42
43
44
45
46

47 **Figure 6.** TRPC6 channels are expressed by metabotropic glutamate receptor type 1a-
48
49 (mGlu_{1a}) or parvalbumin-immunopositive interneurons in the hippocampus. Double
50
51 immunofluorescent staining indicates that both at the border of alveus and stratum oriens, as
52
53 well as in the hilus, the majority of mGlu_{1a}-immunoreactive dendrites also express TRPC6
54
55 (white arrows). In the stratum radiatum, some parvalbumin-containing dendrites are also
56
57
58
59
60

1
2
3 immunoreactive for TRPC6 (white arrows). Arrowheads show singly-immunoreactive
4
5 profiles, colour-coded in the merged pictures. Scale bars: A, D, 10 μm ; G, 5 μm .
6
7
8

9
10 **Figure 7.** Plasma membranes of interneuron dendrites are decorated with immunogold
11 staining representing TRPC6 channels. A1-2. Consecutive images taken in the stratum oriens
12 demonstrate that TRPC6 channels depicted by gold particles (arrows) are present on the
13 plasma membrane of horizontal interneuron dendrites bearing long spines and receiving
14 asymmetric synapses on their shafts and spines (open arrowheads). B: Interneuron dendrites
15 in the hilus receiving asymmetric synapses on their shafts and spines (open arrowheads) are
16 decorated with immunogold labeling. C: On the plasma membrane of an interneuron dendrite
17 in the stratum radiatum densely covered by asymmetric synapses (open arrowheads), which is
18 a hallmark of parvalbumin-expressing interneurons, gold particles are attached to the
19 intracellular surface of the plasma membrane (arrows). Scale bars: 0.5 μm .
20
21
22
23
24
25
26
27
28
29
30
31
32
33
34
35
36
37
38
39
40
41
42
43
44
45
46
47
48
49
50
51
52
53
54
55
56
57
58
59
60

Reference list

- Abramowitz J, Birnbaumer L (2009) Physiology and pathophysiology of canonical transient receptor potential channels. *FASEB J* 23:297-328.
- Acsády L, Kamondi A, Sik A, Freund T, Buzsáki G (1998) GABAergic cells are the major postsynaptic targets of mossy fibers in the rat hippocampus. *J Neurosci* 18:3386-3403.
- Aires V, Hichami A, Boulay G, Khan NA (2007) Activation of TRPC6 calcium channels by diacylglycerol (DAG)-containing arachidonic acid: a comparative study with DAG-containing docosahexaenoic acid. *Biochimie* 89:926-937.
- Amaral DG, Ishizuka N, Claiborne B (1990) Neurons, numbers and the hippocampal network. *Progress in brain research* 83:1-11.
- Bardell TK, Barker EL (2010) Activation of TRPC6 channels promotes endocannabinoid biosynthesis in neuronal CAD cells. *Neurochem Int* 57:76-83.
- Baude A, Nusser Z, David J, Roberts B, Mulvihill E, McIlhinney RAJ, Somogyi P (1993) The metabotropic glutamate receptor (mGluR1) is concentrated at perisynaptic membrane of neuronal subpopulations as detected by immunogold reaction. *Neuron* 11:771-787.
- Bird CM, Burgess N (2008) The hippocampus and memory: insights from spatial processing. *Nature reviews. Neuroscience* 9:182-194.
- Bisogno T, Howell F, Williams G, Minassi A, Cascio MG, Ligresti A, Matias I, Schiano-Moriello A, Paul P, Williams EJ, Gangadharan U, Hobbs C, Di Marzo V, Doherty P (2003) Cloning of the first sn1-DAG lipases points to the spatial and temporal regulation of endocannabinoid signaling in the brain. *J Cell Biol* 163:463-468.
- Blasco-Ibanez JM, Freund TF (1995) Synaptic input of horizontal interneurons in stratum oriens of the hippocampal CA1 subfield: structural basis of feed-back activation. *Eur J neurosci* 7:2170-2180.
- Bollimuntha S, Selvaraj S, Singh BB (2011) Emerging roles of canonical TRP channels in neuronal function. *Advances in experimental medicine and biology* 704:573-593.
- Cahalan MD (2009) STIMulating store-operated Ca(2+) entry. *Nat Cell Biol* 11:669-677.
- Cea-del Rio CA, Lawrence JJ, Tricoire L, Erdelyi F, Szabo G, McBain CJ (2010) M3 muscarinic acetylcholine receptor expression confers differential cholinergic

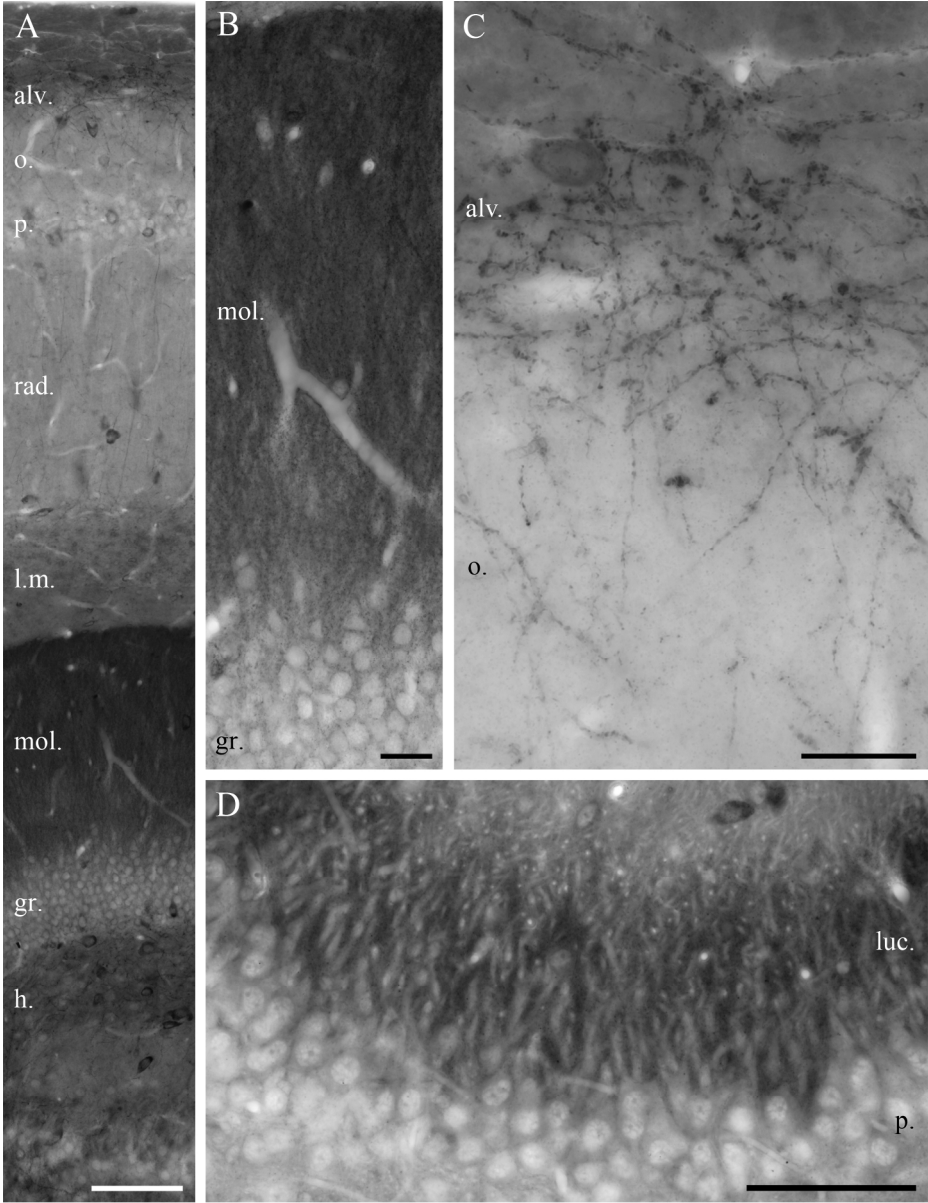
- 1
2
3 modulation to neurochemically distinct hippocampal basket cell subtypes. *The Journal*
4 *of neuroscience* 30:6011-6024.
5
6
7 Chung YH, Sun Ahn H, Kim D, Hoon Shin D, Su Kim S, Yong Kim K, Bok Lee W, Ik Cha C
8 (2006) Immunohistochemical study on the distribution of TRPC channels in the rat
9 hippocampus. *Brain Res* 1085:132-137.
10
11
12 Clapham DE (2003) TRP channels as cellular sensors. *Nature* 426:517-524.
13
14
15 Cope DW, Maccaferri G, Marton LF, Roberts JD, Cobden PM, Somogyi P (2002)
16 Cholecystokinin-immunopositive basket and Schaffer collateral-associated
17 interneurons target different domains of pyramidal cells in the CA1 area of the rat
18 hippocampus. *Neuroscience* 109:63-80.
19
20
21 Dietrich A, Mederos YSM, Gollasch M, Gross V, Storch U, Dubrovskaja G, Obst M, Yildirim
22 E, Salanova B, Kalwa H, Essin K, Pinkenburg O, Luft FC, Gudermann T, Birnbaumer
23 L (2005) Increased vascular smooth muscle contractility in TRPC6^{-/-} mice. *Mol Cell*
24 *Biol* 25:6980-6989.
25
26
27
28 Drake CT, Milner TA, Patterson SL (1999) Ultrastructural localization of full-length trkB
29 immunoreactivity in rat hippocampus suggests multiple roles in modulating activity-
30 dependent synaptic plasticity. *The Journal of neuroscience* 19:8009-8026.
31
32
33 Ferraguti F, Cobden P, Pollard M, Cope D, Shigemoto R, Watanabe M, Somogyi P (2004)
34 Immunolocalization of metabotropic glutamate receptor 1 alpha (mGluR1alpha) in
35 distinct classes of interneuron in the CA1 region of the rat hippocampus.
36 *Hippocampus* 14:193-215.
37
38
39
40 Freund TF, Buzsáki G (1996) Interneurons of the hippocampus. *Hippocampus* 6:345 - 470.
41
42
43 Freund TF, Katona I (2007) Perisomatic inhibition. *Neuron* 56:33-42.
44
45
46 Fukaya M, Uchigashima M, Nomura S, Hasegawa Y, Kikuchi H, Watanabe M (2008)
47 Predominant expression of phospholipase Cbeta1 in telencephalic principal neurons
48 and cerebellar interneurons, and its close association with related signaling molecules
49 in somatodendritic neuronal elements. *The European journal of neuroscience* 28:1744-
50 1759.
51
52
53 Gee CE, Benquet P, Gerber U (2003) Group I metabotropic glutamate receptors activate a
54 calcium-sensitive transient receptor potential-like conductance in rat hippocampus. *J*
55 *Physiol* 546:655-664.
56
57
58
59
60

- 1
2
3
4 Glickfeld LL, Scanziani M (2006) Distinct timing in the activity of cannabinoid-sensitive and
5 cannabinoid-insensitive basket cells. *Nat Neurosci* 9:807-815.
6
7
8 Greka A, Navarro B, Oancea E, Duggan A, Clapham DE (2003) TRPC5 is a regulator of
9 hippocampal neurite length and growth cone morphology. *Nat Neurosci* 6:837-845.
10
11
12 Gulyas AI, Megias M, Emri Z, Freund TF (1999) Total number and ratio of excitatory and
13 inhibitory synapses converging onto single interneurons of different types in the CA1
14 area of the rat hippocampus. *The Journal of neuroscience* 19:10082-10097.
15
16
17 Hofmann T, Obukhov AG, Schaefer M, Harteneck C, Gudermann T, Schultz G (1999) Direct
18 activation of human TRPC6 and TRPC3 channels by diacylglycerol. *Nature* 397:259-
19 263.
20
21
22 Holm MM, Nieto-Gonzalez JL, Vardya I, Vaegter CB, Nykjaer A, Jensen K (2009) Mature
23 BDNF, but not proBDNF, reduces excitability of fast-spiking interneurons in mouse
24 dentate gyrus. *The Journal of neuroscience* 29:12412-12418.
25
26
27 Kano M, Ohno-Shosaku T, Hashimotodani Y, Uchigashima M, Watanabe M (2009)
28 Endocannabinoid-mediated control of synaptic transmission. *Physiological reviews*
29 89:309-380.
30
31
32 Katona I, Acsady L, Freund TF (1999) Postsynaptic targets of somatostatin-immunoreactive
33 interneurons in the rat hippocampus. *Neuroscience* 88:37-55.
34
35
36 Katona I, Freund TF (2008) Endocannabinoid signaling as a synaptic circuit breaker in
37 neurological disease. *Nature medicine* 14:923-930.
38
39
40 Katona I, Urban GM, Wallace M, Ledent C, Jung KM, Piomelli D, Mackie K, Freund TF
41 (2006) Molecular composition of the endocannabinoid system at glutamatergic
42 synapses. *J Neurosci* 26:5628-5637.
43
44
45 Katsumaru H, Kosaka T, Heizmann CW, Hama K (1988) Immunocytochemical study of
46 GABAergic neurons containing the calcium-binding protein parvalbumin in the rat
47 hippocampus. *Exp. Brain Res.* 72:347-362.
48
49
50 Klausberger T, Marton LF, O'Neill J, Huck JH, Dalezios Y, Fuentealba P, Suen WY, Papp E,
51 Kaneko T, Watanabe M, Csicsvari J, Somogyi P (2005) Complementary roles of
52 cholecystokinin- and parvalbumin-expressing GABAergic neurons in hippocampal
53 network oscillations. *The Journal of neuroscience* 25:9782-9793.
54
55
56
57
58
59
60

- 1
2
3
4 Lawrence JJ, Statland JM, Grinspan ZM, McBain CJ (2006) Cell type-specific dependence of
5 muscarinic signalling in mouse hippocampal stratum oriens interneurons. *J Physiol*
6 570:595-610.
7
8
9 Lovett-Barron M, Turi GF, Kaifosh P, Lee PH, Bolze F, Sun XH, Nicoud JF, Zemelman BV,
10 Sternson SM, Losonczy A (2012) Regulation of neuronal input transformations by
11 tunable dendritic inhibition. *Nat Neurosci* 15:769-775.
12
13
14 Lujan R, Nusser Z, Roberts JD, Shigemoto R, Somogyi P (1996) Perisynaptic location of
15 metabotropic glutamate receptors mGluR1 and mGluR5 on dendrites and dendritic
16 spines in the rat hippocampus. *Eur J Neurosci* 8:1488-1500.
17
18
19 Lujan R, Roberts JD, Shigemoto R, Ohishi H, Somogyi P (1997) Differential plasma
20 membrane distribution of metabotropic glutamate receptors mGluR1 alpha, mGluR2
21 and mGluR5, relative to neurotransmitter release sites. *J Chem Neuroanat* 13:219-241.
22
23
24
25 Maccaferri G, McBain CJ (1995) Passive propagation of LTD to stratum oriens-alveus
26 inhibitory neurons modulates the temporoammonic input to the hippocampal CA1
27 region. *Neuron* 15:137-145.
28
29
30 Miles R, Toth K, Gulyás AI, Hajos N, Freund TF (1996) Differences between somatic and
31 dendritic inhibition in the hippocampus. *Neuron* 16:815-823.
32
33
34 Nakamura M, Sato K, Fukaya M, Araishi K, Aiba A, Kano M, Watanabe M (2004) Signaling
35 complex formation of phospholipase Cbeta4 with metabotropic glutamate receptor
36 type 1alpha and 1,4,5-trisphosphate receptor at the perisynapse and endoplasmic
37 reticulum in the mouse brain. *The European journal of neuroscience* 20:2929-2944.
38
39
40 Owsianik G, D'Hoedt D, Voets T, Nilius B (2006) Structure-function relationship of the TRP
41 channel superfamily. *Rev Physiol Biochem Pharmacol* 156:61-90.
42
43
44 Pani B, Bollimuntha S, Singh BB (2012) The TR (i)P to Ca²⁺ signaling just got STIMy: an
45 update on STIM1 activated TRPC channels. *Front Biosci* 17:805-823.
46
47
48 Pouille F, Scanziani M (2004) Routing of spike series by dynamic circuits in the
49 hippocampus. *Nature* 429:717-723.
50
51
52
53 Ramsey IS, Delling M, Clapham DE (2006) An introduction to TRP channels. *Annual review*
54 *of physiology* 68:619-647.
55
56
57
58
59
60

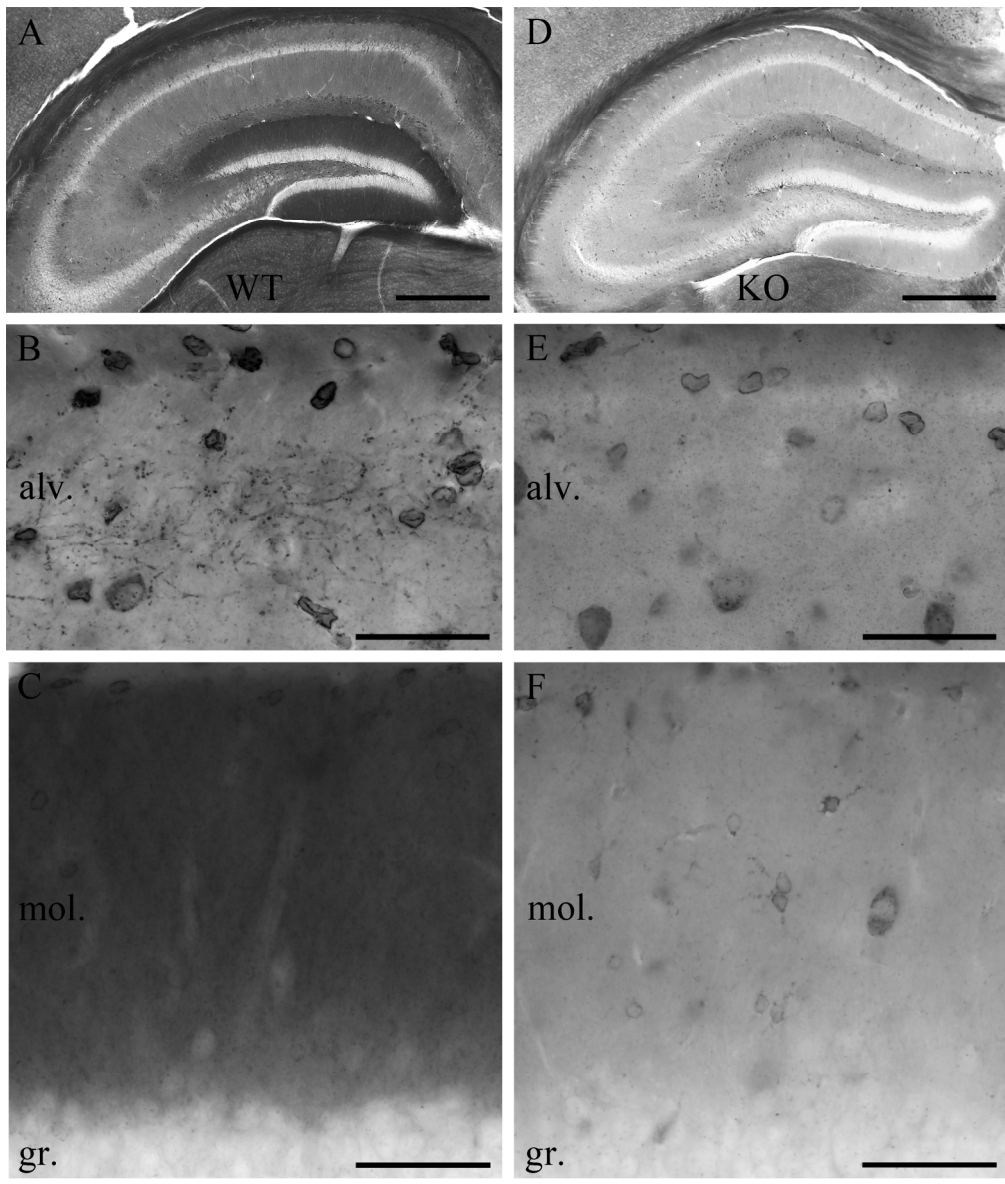
- 1
2
3 Shimizu H, Fukaya M, Yamasaki M, Watanabe M, Manabe T, Kamiya H (2008) Use-
4 dependent amplification of presynaptic Ca²⁺ signaling by axonal ryanodine receptors
5 at the hippocampal mossy fiber synapse. *Proc Natl Acad Sci U S A* 105:11998-12003.
6
7
8 Tai Y, Feng S, Ge R, Du W, Zhang X, He Z, Wang Y (2008) TRPC6 channels promote
9 dendritic growth via the CaMKIV-CREB pathway. *J Cell Sci* 121:2301-2307.
10
11
12 Takacs VT, Klausberger T, Somogyi P, Freund TF, Gulyas AI (2012) Extrinsic and local
13 glutamatergic inputs of the rat hippocampal CA1 area differentially innervate
14 pyramidal cells and interneurons. *Hippocampus* 22:1379-1391.
15
16
17 Tanaka J, Nakagawa S, Kushiya E, Yamasaki M, Fukaya M, Iwanaga T, Simon MI, Sakimura
18 K, Kano M, Watanabe M (2000) Gq protein alpha subunits Galphaq and Galpha11 are
19 localized at postsynaptic extra-junctional membrane of cerebellar Purkinje cells and
20 hippocampal pyramidal cells. *The European journal of neuroscience* 12:781-792.
21
22
23 Topolnik L, Azzi M, Morin F, Kougioumoutzakis A, Lacaille JC (2006) mGluR1/5 subtype-
24 specific calcium signalling and induction of long-term potentiation in rat hippocampal
25 oriens/alveus interneurons. *J Physiol* 575:115-131.
26
27
28
29 Uchigashima M, Narushima M, Fukaya M, Katona I, Kano M, Watanabe M (2007)
30 Subcellular arrangement of molecules for 2-arachidonoyl-glycerol-mediated
31 retrograde signaling and its physiological contribution to synaptic modulation in the
32 striatum. *The Journal of neuroscience* 27:3663-3676.
33
34
35 van Hoof JA, Giuffrida R, Blatow M, Monyer H (2000) Differential expression of group I
36 metabotropic glutamate receptors in functionally distinct hippocampal interneurons.
37 *The Journal of neuroscience* 20:3544-3551.
38
39
40 Yamasaki M, Matsui M, Watanabe M (2010) Preferential localization of muscarinic M1
41 receptor on dendritic shaft and spine of cortical pyramidal cells and its anatomical
42 evidence for volume transmission. *The Journal of neuroscience* 30:4408-4418.
43
44
45
46 Yoshida T, Fukaya M, Uchigashima M, Miura E, Kamiya H, Kano M, Watanabe M (2006)
47 Localization of diacylglycerol lipase-alpha around postsynaptic spine suggests close
48 proximity between production site of an endocannabinoid, 2-arachidonoyl-glycerol,
49 and presynaptic cannabinoid CB1 receptor. *J Neurosci* 26:4740-4751.
50
51
52 Zhou J, Du W, Zhou K, Tai Y, Yao H, Jia Y, Ding Y, Wang Y (2008) Critical role of TRPC6
53 channels in the formation of excitatory synapses. *Nat Neurosci* 11:741-743.
54
55
56
57
58
59
60

1
2
3
4
5
6
7
8
9
10
11
12
13
14
15
16
17
18
19
20
21
22
23
24
25
26
27
28
29
30
31
32
33
34
35
36
37
38
39
40
41
42
43
44
45
46
47
48
49
50
51
52
53
54
55
56
57
58
59
60



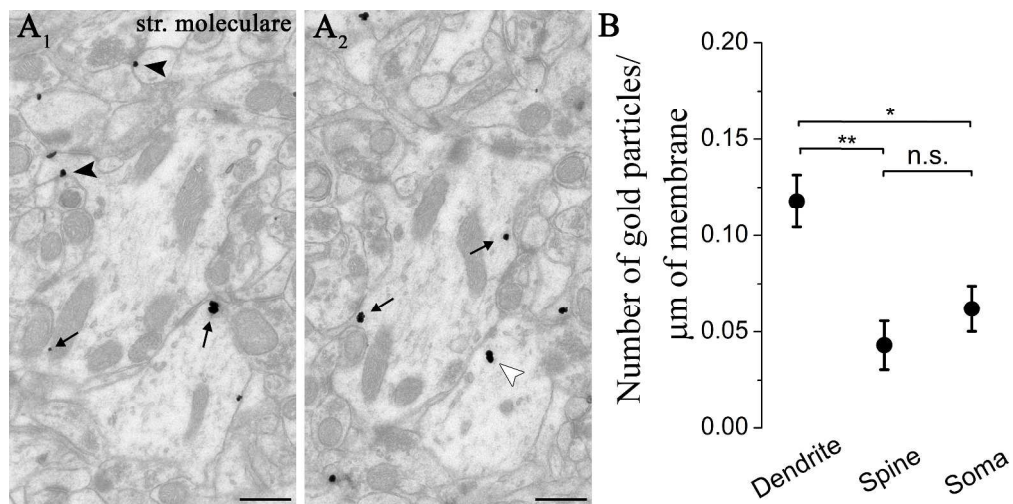
189x245mm (300 x 300 DPI)

1
2
3
4
5
6
7
8
9
10
11
12
13
14
15
16
17
18
19
20
21
22
23
24
25
26
27
28
29
30
31
32
33
34
35
36
37
38
39
40
41
42
43
44
45
46
47
48
49
50
51
52
53
54
55
56
57
58
59
60



189x222mm (300 x 300 DPI)

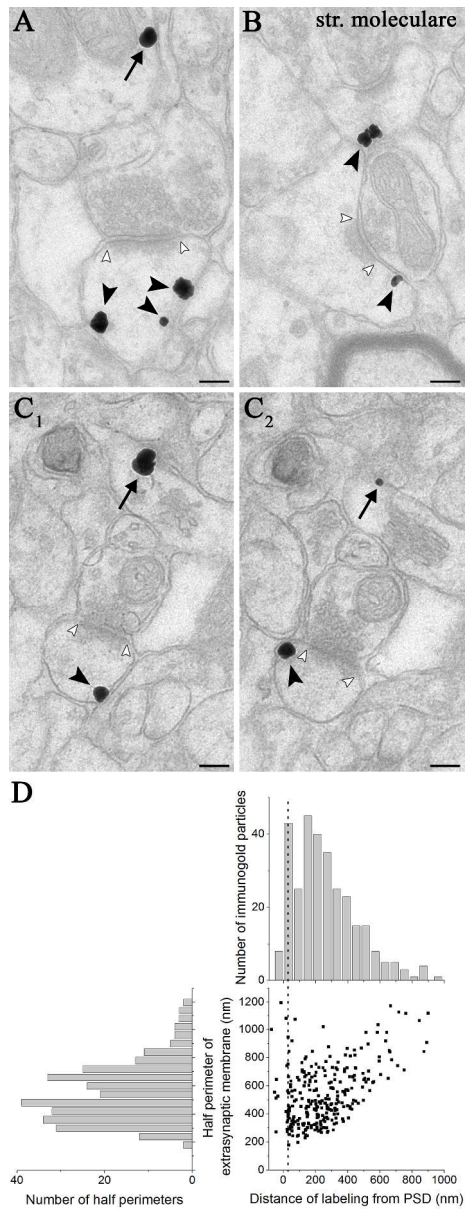
1
2
3
4
5
6
7
8
9
10
11
12
13
14
15
16
17
18
19
20
21
22
23
24
25
26
27
28
29
30
31
32
33
34
35
36
37
38
39
40
41
42
43
44
45
46
47
48
49
50
51
52
53
54
55
56
57
58
59
60



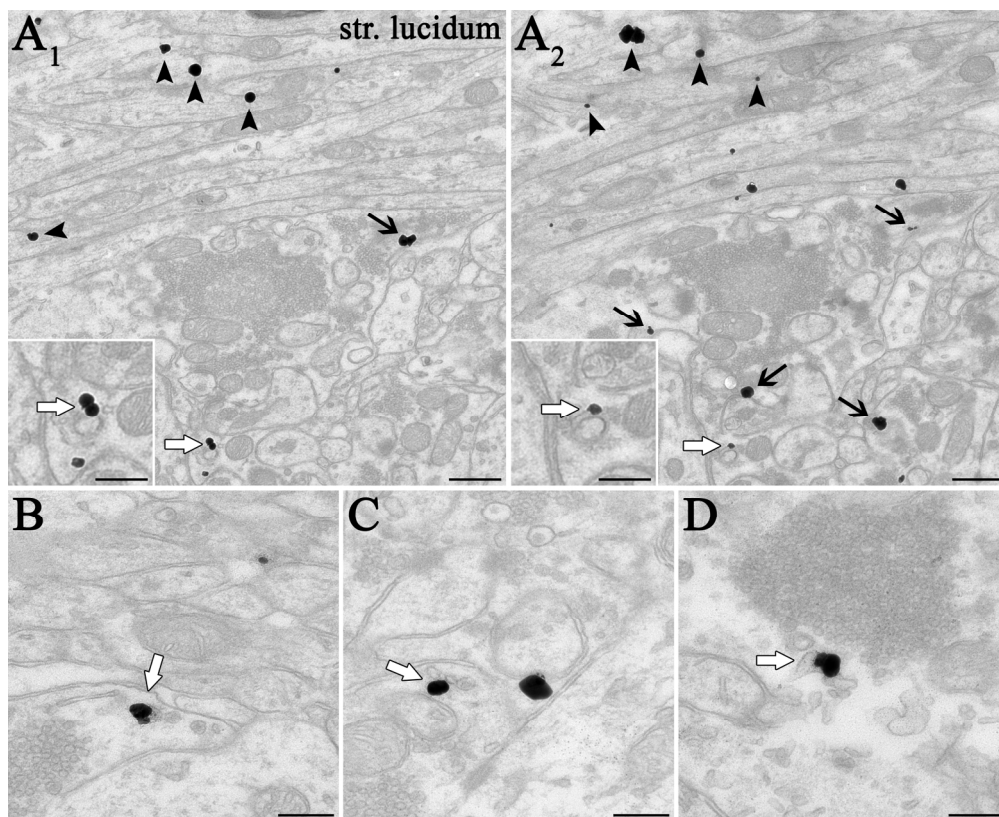
342x169mm (300 x 300 DPI)

Peer Review

1
2
3
4
5
6
7
8
9
10
11
12
13
14
15
16
17
18
19
20
21
22
23
24
25
26
27
28
29
30
31
32
33
34
35
36
37
38
39
40
41
42
43
44
45
46
47
48
49
50
51
52
53
54
55
56
57
58
59
60



171x454mm (300 x 300 DPI)

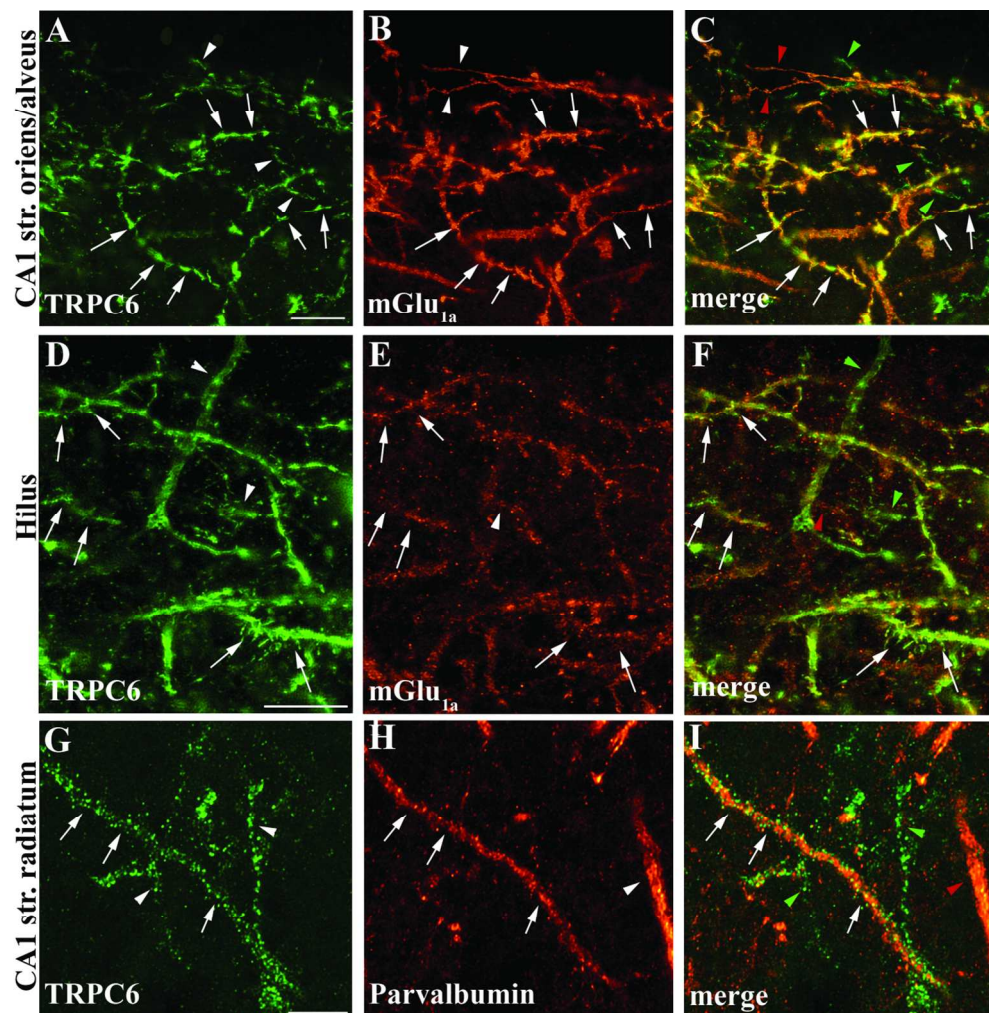


175x142mm (300 x 300 DPI)

Review

1
2
3
4
5
6
7
8
9
10
11
12
13
14
15
16
17
18
19
20
21
22
23
24
25
26
27
28
29
30
31
32
33
34
35
36
37
38
39
40
41
42
43
44
45
46
47
48
49
50
51
52
53
54
55
56
57
58
59
60

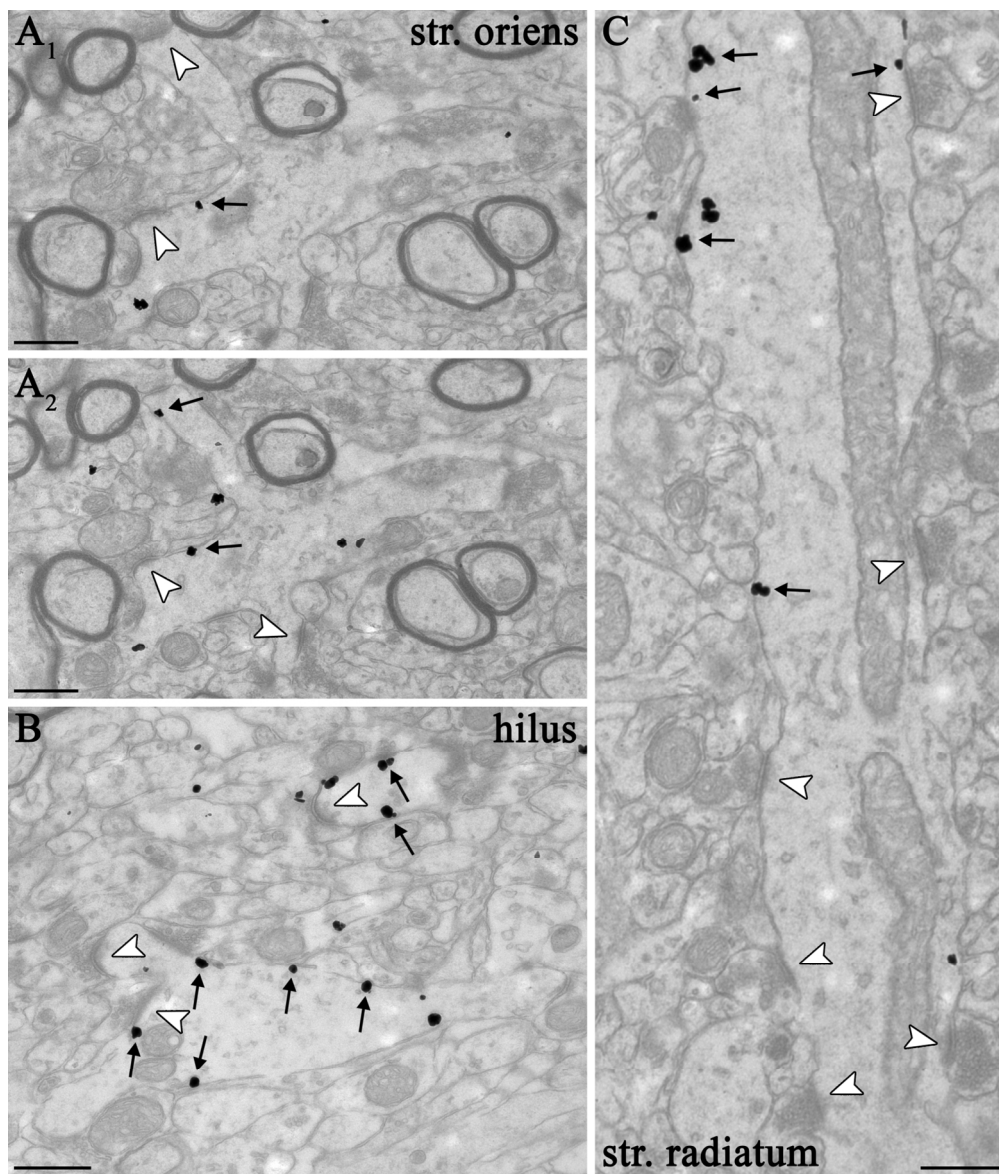
1
2
3
4
5
6
7
8
9
10
11
12
13
14
15
16
17
18
19
20
21
22
23
24
25
26
27
28
29
30
31
32
33
34
35
36
37
38
39
40
41
42
43
44
45
46
47
48
49
50
51
52
53
54
55
56
57
58
59
60



118x119mm (300 x 300 DPI)



1
2
3
4
5
6
7
8
9
10
11
12
13
14
15
16
17
18
19
20
21
22
23
24
25
26
27
28
29
30
31
32
33
34
35
36
37
38
39
40
41
42
43
44
45
46
47
48
49
50
51
52
53
54
55
56
57
58
59
60



139x161mm (300 x 300 DPI)